

Registered Office

Herrmann-Debrouxlaan 40
1160 Brussel – Belgium

Foundation of Public Utility

VAT BE 406.568.867

Research Centres

Boeretang 200
2400 Mol – Belgium

Chemin du Cyclotron 6

1348 Ottignies-Louvain-la-Neuve – Belgium

Reference N°	Creation Date	
SCK CEN/44994558	2021-08-19	
Alternative Reference N°	Revision	Version
N/A	1.0	1
ISC	Revision Status	
Public	Approved	

Proceedings 4th International Rilem Conference 2021-05-06 A Continuum Model for Carbonation Curing of Fiber-Cement Composites

Authors*

Quoc Tri Phung

Approval information for current revision*

Name	Outcome	Date
Janez Perko	Approved	2021-08-25

Change log*

Revision	Version	Status	Date	Description of change
1.0	1	Approved	2021-08-19	

**This automatically generated cover page shows references and document information as were available in the Alexandria document management system on 2021-08-25. Please refer to Alexandria for current and complete metadata, or to the document contents and/or author for additional information.*



A CONTINUUM MODEL FOR CARBONATION CURING OF FIBER-CEMENT COMPOSITES

S.C. Seetharam(1), Q.T. Phung(1), B. Kottititum(2), N. Maes(1), T. Srinophakun(2)

(1) Belgian Nuclear Research Centre (SCK•CEN), 2400 Mol, Belgium

(2) Department of Chemical Engineering, Kasetsart University, Bangkok, Thailand

Abstract

Accelerated carbonation curing of cellulose fiber-cement composites is known to improve their durability in the form of decreased porosity and increased mechanical properties. In addition, because carbonation results in a decrease in the alkalinity of cement paste, it makes cement less aggressive towards the cellulose fibers. The properties of the composite can be controlled by adjusting carbonation curing time, carbonation curing pressure as well as mechanical rolling pressure. In this context, a continuum model is proposed that couples the process of hydration of cement with heat, moisture and CO₂ transport, including precipitation of CaCO₃, change of porosity because of hydration as well as carbonation and water release and consumption. Experimental data on carbonation curing of a cellulose fiber-cement composite has recently become available, which serves to validate the model. Preliminary results indicate that the model is able to predict within reasonable accuracy the depth of carbonation.

Keywords: Carbonation, Hydration, Fiber-cement composites, Modelling, Early age

1. INTRODUCTION

The carbonation process in hardened cement-based materials is typically considered as a deterioration phenomenon because it results in a pH decrease, which accelerates the corrosion of reinforcing bars in concrete. On the other hand, carbonation also results in beneficial effects such as decrease in transport properties, refined pore structure of cement-based materials [1, 2], and enhanced mechanical properties, which is frequently applied to improve the performance of fiber-cement composites properties. Typically, fiber-cement composites have high porosity resulting in low physical and mechanical properties. Accelerated carbonation of fiber-cement matrix during the curing period significantly enhances their durability [3]. The extent of modification in microstructure and hence mechanical properties significantly depends on carbonation conditions (e.g. CO₂ concentration, relative humidity, applied CO₂ pressure) and cement types (e.g. OPC or blended systems) and the age of materials. The reduction of transport properties is a result of the precipitation of carbonation products in the pore structure, which leads to a significant reduction of the total porosity [4].

Typically, hydration is not considered in carbonation models because the hydration is nearly stable in hardened materials (after 28-day curing), which is not the case for early age carbonation curing of fiber-cement composites (carbonation typically initiated few hours after casting). In a previous study [5], the authors have successfully developed a comprehensive 1D reactive transport model accounting for both advective and diffusive transports under CO₂ pressure gradients for hardened cement pastes. This model enables to predict carbonation depth and changes in permeability, diffusivity, and porosity due to carbonation. In this study, an improved model is proposed that couples the process of hydration of cement with heat, moisture and CO₂ transport in order to investigate the key parameters including curing time, curing pressure, rolling pressure and initial physical properties of fiber-cement composites on the carbonation efficiency. The performance of the model is explored by simulating an accelerated carbonation curing experiment reported in [6].

2. COUPLED MODEL

2.1 Hydration of fiber-cement composites

This study considers reactions of four main cement clinker phases (i.e. C₃S, C₂S, C₃A, C₄AF) with water as shown in Table 1. Fibers and limestone filler are considered as inert ingredients. The rate equations are based on Papadakis et al. [7], which are empirical. The effect of temperature is also considered by correcting the hydration rate constant using Arrhenius equation.

Table 1: Hydration and carbonation reactions considered in the model

Hydration reactions	
$3\text{CaO} \cdot \text{SiO}_2 + 4.3\text{H}_2\text{O} \xrightarrow{r_{\text{H,C3S}}} 1.7\text{CaO} \cdot \text{SiO}_2 \cdot 3\text{H}_2\text{O} + 1.3\text{Ca}(\text{OH})_2$	(1)
$2\text{CaO} \cdot \text{SiO}_2 + 3.3\text{H}_2\text{O} \xrightarrow{r_{\text{H,C2S}}} 1.7\text{CaO} \cdot \text{SiO}_2 \cdot 3\text{H}_2\text{O} + 0.3\text{Ca}(\text{OH})_2$	(2)
$3\text{CaO} \cdot \text{Al}_2\text{O}_3 + 3\text{CaSO}_4 \cdot 2\text{H}_2\text{O} + 26\text{H}_2\text{O} \xrightarrow{r_{\text{H,C3A,S}}} 3\text{CaO} \cdot \text{Al}_2\text{O}_3 \cdot 3\text{CaSO}_4 \cdot 32\text{H}_2\text{O}$	(3)
$4\text{CaO} \cdot \text{Al}_2\text{O}_3 \cdot \text{Fe}_2\text{O}_3 + 2\text{Ca}(\text{OH})_2 + 2(\text{CaSO}_4 \cdot 2\text{H}_2\text{O}) + 18\text{H}_2\text{O} \xrightarrow{r_{\text{H,C4AF,S}}} 6\text{CaO} \cdot \text{Al}_2\text{O}_3 \cdot \text{Fe}_2\text{O}_3 \cdot 2\text{CaSO}_4 \cdot 24\text{H}_2\text{O}$	(4)
$3\text{CaO} \cdot \text{Al}_2\text{O}_3 + \text{Ca}(\text{OH})_2 + 12\text{H}_2\text{O} \xrightarrow{r_{\text{H,C3A}}} 3\text{CaO} \cdot \text{Al}_2\text{O}_3 \cdot \text{Ca}(\text{OH})_2 \cdot 12\text{H}_2\text{O}$	(5)
$4\text{CaO} \cdot \text{Al}_2\text{O}_3 \cdot \text{Fe}_2\text{O}_3 + 2\text{Ca}(\text{OH})_2 + 22\text{H}_2\text{O} \xrightarrow{r_{\text{H,C4AF}}} 6\text{CaO} \cdot \text{Al}_2\text{O}_3 \cdot \text{Fe}_2\text{O}_3 \cdot 2\text{Ca}(\text{OH})_2 \cdot 24\text{H}_2\text{O}$	(6)
Carbonation reactions	
$3\text{CaO} \cdot \text{SiO}_2 + 3\text{CO}_2(\text{aq}) + (\text{H}_2\text{O}) \xrightarrow{r_{\text{C3S}}} \text{SiO}_2 + (\text{H}_2\text{O}) + 3\text{CaCO}_3$	(7)
$2\text{CaO} \cdot \text{SiO}_2 + 2\text{CO}_2(\text{aq}) + (\text{H}_2\text{O}) \xrightarrow{r_{\text{C2S}}} \text{SiO}_2 + (\text{H}_2\text{O}) + 2\text{CaCO}_3$	(8)
$1.7\text{CaO} \cdot \text{SiO}_2 \cdot 3\text{H}_2\text{O} + 1.7\text{CO}_2(\text{aq}) \xrightarrow{r_{\text{CSH}}} 1.7\text{CaCO}_3 + \text{SiO}_2 \cdot 1.8\text{H}_2\text{O} + 1.2\text{H}_2\text{O}$	(9)
$3\text{CaO} \cdot \text{Al}_2\text{O}_3 \cdot 3\text{CaSO}_4 \cdot 32\text{H}_2\text{O} + 3\text{CO}_2(\text{aq}) \xrightarrow{r_{\text{AFt}}} 3\text{CaCO}_3 + 3\text{CaSO}_4 \cdot 2\text{H}_2\text{O} + 2\text{Al}(\text{OH})_3 + 9\text{H}_2\text{O}$	(10)
$\text{Ca}(\text{OH})_2(\text{aq}) + \text{CO}_2(\text{aq}) \xrightarrow{r_{\text{CH}}} \text{CaCO}_3 + \text{H}_2\text{O}$	(11)

2.2 Carbonation at early age under CO₂ curing

Among the hydration products, calcium silicate hydrate (C-S-H), portlandite (CH), and ettringite (AFt) undergo carbonation. Furthermore, two main clinkers (i.e. C₂S and C₃S), which have not yet hydrated, are also carbonated as shown in Table 1. The carbonation reactions occur in the aqueous phase, which involve both dissolution of solid phases and their reaction with dissolved CO₂. The kinetics of these carbonation reactions are therefore expressed using a first

order rate equation comprising dissolved CO₂ concentration and exposed surface area of reactive solid phases [8].

2.3 Transport of heat, moisture and CO₂

The formulation for coupled heat and moisture (liquid and vapour) transport is based on Thomas and Ye [9] and references therein, with the deviation that the moisture transport is recast in terms of relative humidity (RH) as the primary variable. Note that heat convection is ignored. As heat is generated because of hydration, the heat transfer equation additionally considers a heat source term [9]. The formulation for two-phase transport of CO₂ (gaseous and aqueous) is based on Phung et al. [5] and references therein. The water release due to carbonation and water consumption due to hydration (Table 1) is incorporated as a sink/source term in the moisture transport equation [9].

2.5 Evolution of porosity during hydration and carbonation

The change in porosity is obtained from the change in solid phases produced by the hydration of cement clinkers and carbonation of hydration products and unhydrated clinkers (C₂S, C₃S). The total porosity, ϕ , of a sample during carbonation is expressed as follows:

$$\phi = \phi_0 - \sum ([i]_0 - [i]) \Delta \bar{V}_{H,i} - \sum (CC_i) \Delta \bar{V}_{CC,i} \quad (12)$$

where ϕ_0 is the initial total porosity. i_0 and i are the concentration of cement species at initial and any time step during hydration. CC_i is the concentration of calcium carbonate attributable to reactant i during carbonation. $\Delta \bar{V}_{H,i}$ and $\Delta \bar{V}_{CC,i}$ are the change in volume per mole of reactant i during hydration and carbonation, respectively. The carbonation of hydration product might partially contribute to the capillary porosity change, especially under accelerated conditions. Following the previous study [5], the capillary porosity is calculated as follows:

$$\phi_c = \phi_h + 0.5 \sum (CC_i) \Delta \bar{V}_{CC,i} \quad (13)$$

where ϕ_h is the capillary porosity due to hydration, which can be estimated based on hydration degree.

3. APPLICATION

3.1 Accelerated carbonation curing experiments

A dry mixture of fiber-cement composites consisted of 75% OPC type I cement, 20% limestone filler, 3% cellulose fiber, and 1% synthetic fiber PVA. The water to cement ratio was initially controlled at 0.62, which reduced to 0.45 and 0.45 after passing through the Hatschek rolling machine at rolling pressure of 2.5 bar and 9 bar, respectively. After 3 hours since casting, the fiber-cement composite samples (70 mm × 210 mm × 5 mm) were placed in a carbonation chamber under semi-adiabatic conditions for 3, 5, and 9 h at different CO₂ pressures (1 and 3 bar). After that, they were kept in air saturated curing condition (i.e., sealed in plastic bags) under 25 °C until 3, 7, 14, and 28 days of age. CO₂ of approximately 99.5% purity was injected to the carbonation chamber, which contained a stack of 15 samples. Temperature and relative humidity inside the chamber were measured during carbonation. Details of the experiments are available in [6].

After carbonation, a number of post-analysis methods were used to qualitatively and quantitatively analyse the carbonated samples including the physical properties (porosity, bulk density) and mechanical properties (not shown in this paper). Furthermore, the carbonated

sample was sawn and sprayed by phenolphthalein solution to determine the phenolphthalein carbonation depth [2]. For simulation purposes, the experiment with a rolling pressure of 9 bar and 9 h carbonation curing is considered.

Table 2: Salient material parameters

Parameter	Value used and source		
Moisture retention	$S = [1 + (-\varepsilon \ln(RH))^{1/(1-\gamma)}]^{-\gamma}$ [5] $\varepsilon = 5.72; \gamma = 0.444$		
Intrinsic permeability	$k_{int} = \zeta_p d_{cr}^2 \phi_c^{2.5} / (1 - \phi_c)$ (m ²) [10] $\zeta_p = 0.0118; d_{cr} = 9 \times 10^{-8}$ (m)		
Hydraulic conductivity	$k_l = k_{int} k_{rl} (g\rho/\mu)$ (m/s) [5] $k_{rl} = S^p [1 - (1 - S^{1/q})^q]^2$; $p = 5.5; q = 0.56$		
Thermal conductivity	2.5 (W/m/K) [11]		
Diffusivity of CO ₂	For dissolved CO ₂ : $D_l = D_{l0} k_{Dl}^*(\phi, \tau) k_{Dl}(S)$ (m ² /s) [5] $k_{Dl}^*(\phi, \tau) = (1 - 0.7d_c) k_{Dl}(\phi, \tau)$ $k_{Dl}(\phi, \tau) = 0.001 + 0.07\phi_c^2 + 1.8H(\phi_c - 0.18)(\phi_c - 0.18)^2$ $k_{Dl}(S) = S^\alpha$; $D_{l0} = 1.94 \times 10^{-9}$ (m ² /s); $\alpha = 3.3$ For CO ₂ gas: $D_g = D_{g0} k_{Dg}^*(\phi, \tau) k_{Dg}(S) k_{Knu}$ (m ² /s) [5] $k_{Dg}^*(\phi, \tau) = (1 - 0.7d_c) k_{Dg}(\phi, \tau)$ $k_{Dg}(\phi, \tau) = \phi^\beta$ $k_{Dg}(S) = (1 - S)^\alpha$ $k_{Knu} = 1/(1 + \Re dc)$ $\Re = 5; \beta = 1.33; d_c = 1$ if portlandite = 0, otherwise $d_c = 0$		
Carbonation rate constants	Phases	Rate constants	
	C ₃ S	10 ⁻⁸ (m/s)	
	C ₂ S	10 ⁻⁹ (m/s)	
	CSH	10 ⁻⁹ (m/s)	
	CH	3.58 × 10 ⁻² (1/s)	
	AFt	10 ⁻⁹ (m/s)	
Hydration rate constants	$Ae^{(-E_a/RT)}$		
	Phases	A (1/s); derived from [12]	E _a (kJ/mol)
	C ₃ S	34.39	36.3
	C ₂ S	166.98	45
	C ₃ A	0.70	25
	C ₄ AF	17.24	35

3.2 Modelling methodology

Numerical analysis have been carried out in a step-wise manner to follow the experimental protocol. In particular, the analysis have been carried out in three steps: (i) first, the hydration reactions of a single sample are modelled assuming equilibrium with ambient conditions (fixed RH and temperature at the boundary of the sample), (ii) second, the combined hydration and carbonation reactions of a stack of 15 samples are modelled assuming a 2D geometry as shown in Figure 1, and (iii) third, only hydration is modelled post carbonation assuming thermal equilibrium with the surroundings and no moisture flux in/out of the sample. The initial conditions for each step is obtained from the preceding step. As for boundary conditions in step 2, zero flux is imposed at the chamber boundary for both CO₂ and moisture, and convective heat loss is allowed at the boundary.

Salient material parameters are principally extracted from literature as shown in Table 2. It is worthwhile to note that no parameters are calibrated in this study.

3.3 Results

This section mainly focusses on the discussion of results for the carbonation step. Figure 1 shows 2D contours of temperature and RH fields at around 6 hours, which corresponds to the simulated peak temperature as shown in Figure 2. The results are consistent with typical experimental observations with the maximum temperature predicted at the centre of the domain due to hydration heat of the samples, and minimum temperature at the walls of the curing chamber. The RH results are consistent with the temperature field. The initial RH in the chamber is initially roughly around 75%, which increases progressively because of water release from carbonation reactions and also from the hydrating samples (high initial moisture content) due to both RH and temperature gradient. The model shows condensation at the inner walls of the chamber, which was also visually observed during the dismantling of the chamber. Figure 2 shows a comparison of simulated and experimental results of the evolution of temperature and RH variables. Note that the simulated values are averaged over the void space in the modelled chamber. The results are qualitatively consistent with the experimental data. Quantitative discrepancy is attributed to the 2D simplification of the problem, averaging of the temperature and RH values in the void space although these fields are not uniform as seen from Figure 1, and any uncertainty in the material parameters.

Figure 3 shows simulated carbonation depth at the end of the curing period (12 hours). The carbonation depth is here assumed to be the region where CH is almost completely consumed. The experimental measurements showed an average carbonation depth of 0.5 mm. The simulated results corresponds well with this value (Figure 3, right).

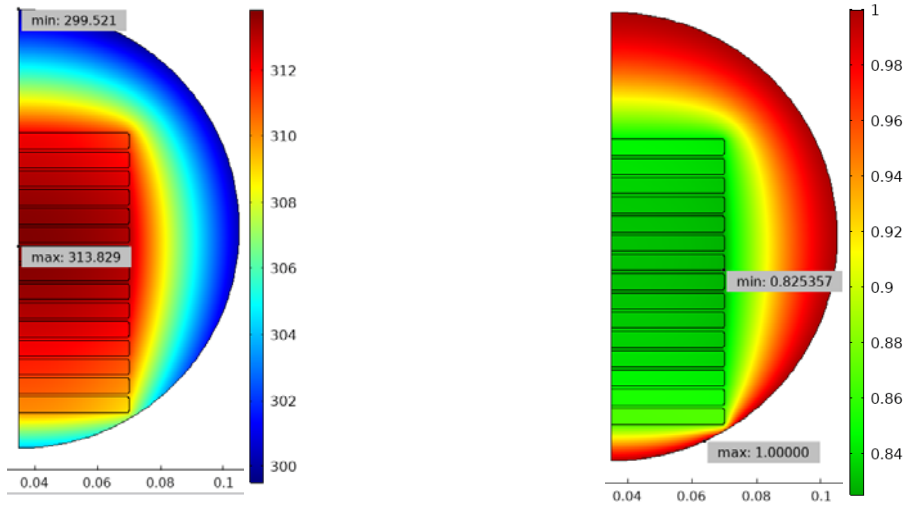


Figure 1: Predicted temperature (left) and RH (right) snapshots at ≈ 6 hours (simulated peak temperature, see Figure 2)

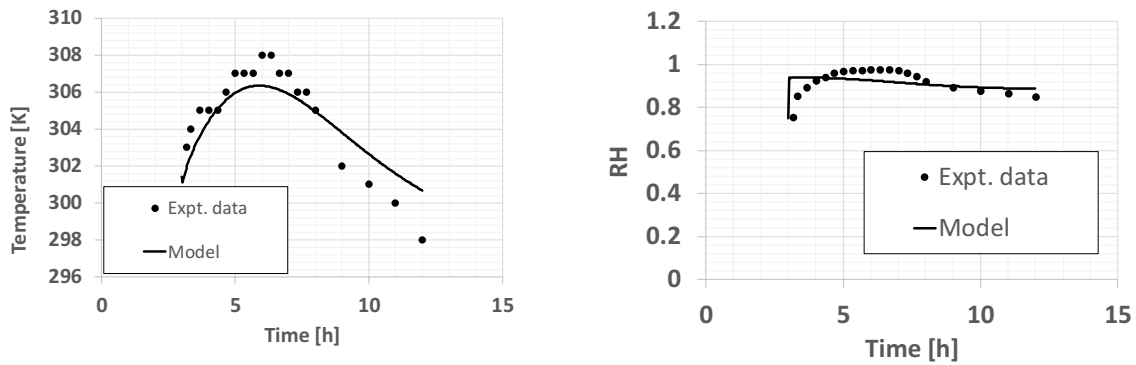


Figure 2: Comparison of experimental vs. predicted results of temperature (left) and RH (right)

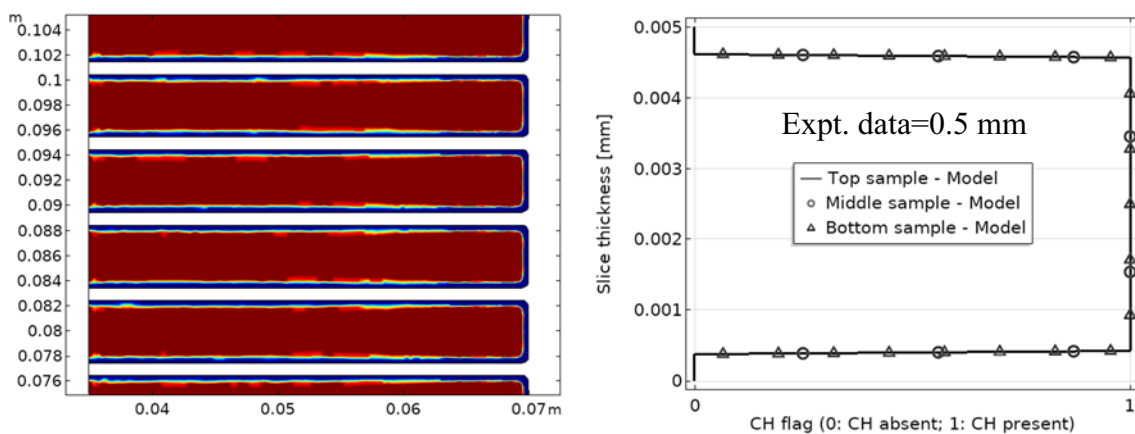


Figure 3: Carbonation penetration depth (equivalent to complete CH consumption)

4. CONCLUSIONS

An improved continuum model is proposed that couples the process of hydration of cement with heat, moisture and CO₂ transport, including precipitation of CaCO₃, change of porosity because of hydration as well as carbonation and water release and consumption. This serves as an invaluable tool to study the influence of key parameters such as curing time, curing pressure, rolling pressure and initial physical properties of fiber-cement composites on the carbonation efficiency. The performance of the model was tested by simulating an accelerated carbonation curing experiment. Qualitatively consistent results were obtained with respect to temperature and RH fields. The model was also able to predict within reasonable accuracy the depth of carbonation. At this point, the main challenge lies in dealing with the uncertainty in the significant number of material parameters in the continuum model.

ACKNOWLEDGEMENTS

This work is supported by SCK•CEN as part of their internal RD&D program on concrete durability.

REFERENCES

- [1] Q.T. Phung, N. Maes, D. Jacques, G.d. Schutter, G. Ye, Effect of Limestone Fillers on Ca-Leaching and Carbonation of Cement Pastes, *Key Engineering Materials*, 711 (2016) 269-276.
- [2] Q.T. Phung, N. Maes, D. Jacques, E. Bruneel, I. Van Driessche, G. Ye, G. De Schutter, Effect of limestone fillers on microstructure and permeability due to carbonation of cement pastes under controlled CO₂ pressure conditions, *Constr Build Mater*, 82 (2015) 376-390.
- [3] G. Tonoli, S. Santos, A. Joaquim, H. Savastano Jr, Effect of accelerated carbonation on cementitious roofing tiles reinforced with lignocellulosic fibre, *Construction and Building Materials*, 24 (2010) 193-201.
- [4] Q.T. Phung, Effects of Carbonation and Calcium Leaching on Microstructure and Transport Properties of Cement Pastes, in: Department of Structural Engineering, Ghent University, Belgium, 2015, pp. 249.
- [5] Q.T. Phung, N. Maes, D. Jacques, G. De Schutter, G. Ye, J. Perko, Modelling the carbonation of cement pastes under a CO₂ pressure gradient considering both diffusive and convective transport, *Constr Build Mater*, 114 (2016) 333-351.
- [6] B. Kottitum, Q.T. Phung, N. Maes, W. Prakaypan, T. Srinophakun, Early Age Carbonation of Fiber-Cement Composites under Real Processing Conditions: A Parametric Investigation, *Applied Sciences*, (2018) 21.
- [7] V.G. Papadakis, C.G. Vayenas, M.N. Fardis, Fundamental Modeling and Experimental Investigation of Concrete Carbonation, *Aci Mater J*, 88 (1991) 363-373.
- [8] M. Peter, A. Muntean, S. Meier, M. Böhm, Competition of several carbonation reactions in concrete: A parametric study, *Cement and Concrete Research*, 38 (2008) 1385-1393.
- [9] H.R. Thomas, Y. He, Analysis of coupled heat, moisture and air transfer in a deformable unsaturated soil, 45 (1995) 677-689.
- [10] Q.T. Phung, N. Maes, D. Jacques, G.D. Schutter, G. Ye, EFFECTS OF W/P RATIO AND LIMESTONE FILLER ON PERMEABILITY OF CEMENT PASTES, in: O.M. Jensen, K. Kovler, N.D. Belie (Eds.) International RILEM Conference Materials, Systems and

Structures in Civil Engineering 2016, RILEM Publications S.A.R.L., Lyngby, Denmark, 2016, pp. 141-151.

- [11] P.K. Mehta, P.J.M. Monteiro, Concrete: microstructure, properties, and materials, McGraw-Hill, 2006.
- [12] V.G. Papadakis, C.G. Vayenas, M.N. Fardis, A Reaction Problem of Engineering Approach to the Concrete Carbonation, Aiche J, 35 (1989) 1639-1650.